

## Efficient visible light photocatalysis in cubic $\text{Sr}_2\text{FeNbO}_6$

E. D. Jeong<sup>a</sup>, S. M. Yu<sup>a</sup>, J. Y. Yoon<sup>a</sup>, J. S. Bae<sup>a</sup>, C. R. Cho<sup>b</sup>, K. T. Lim<sup>c</sup>, Rekha Dom<sup>d</sup>, P. H. Borse<sup>d,\*</sup> and H. G. Kim<sup>a,\*</sup>

<sup>a</sup>Busan Center, Korea Basic Science Institute, Busan 609-735, Korea.

<sup>b</sup>Department of Nano Fusion Technology, Pusan National University, Pusan 609-735, Korea

<sup>c</sup>Department of Imaging System Engineering, Pukyong National University, Busan 609-735, Korea.

<sup>d</sup>Centre for Nanomaterials, International Advanced Research Centre for Powder Metallurgy and New Materials (ARC International), Balapur PO, Hyderabad, AP, 500 005, India.

Cubic phase  $\text{Sr}_2\text{FeNbO}_6$  (SFNO) particles were synthesized and studied experimentally for visible light photocatalysis. The photocatalytic activity for hydrogen (2 times) and oxygen (1.1 times) evolution was very high, as compared to that for  $\text{PbBi}_2\text{Nb}_2\text{O}_9$  (visible light active photocatalysts). As a qualitative guiding tool, a density functional theory study of cubic SFNO demonstrates that the valence band consists of  $\text{O}2p$  hybridized with Nb-states and possibly Fe  $3d$  states (Fe  $3d_{x^2-y^2}$ , Fe  $3d_z^2$ ), while the conduction band mainly consists of Sr  $4d$  states, possibly with Nb  $4d$  as its minima. In particular, the intermediate prominent existence of the Fe  $d$ -orbital expectedly renders a high coefficient of absorption making SFNO a potential visible light active photocatalyst. The qualitative correlation of the experimental results and computed electronic structure affirms its suitability for visible light applications.

**Key words:**  $\text{Sr}_2\text{FeNbO}_6$ , Visible light photocatalysis, Hydrogen evolution, Electronic-structure, Photocatalytic activity.

### Introduction

A double perovskite structured metal oxide  $\text{Sr}_2\text{FeNbO}_6$  has been studied in the past for its photo-electrochemical applications [1, 2] and predicted it to be a potential fuel cell electrode material [3]. It has also been categorized as a useful visible light active photocatalyst for water-splitting [4]. In spite of its suitable band energetics for photoreduction/photooxidation of water, its solar hydrogen energy generation potential has not been analysed in depth. In this investigation, we study theoretically and experimentally, the physico-chemical properties of  $\text{Sr}_2\text{FeNbO}_6$  (SFNO) and further analyze the results to interpret its solar hydrogen generation capability.

The research on the fabrication of an efficient visible light water splitting photocatalyst is in demand due to the predicted energy crises that would be faced by vanishing fossil fuels on earth. The best known photocatalysts [5, 6], binary or ternary metal oxides:  $\text{TiO}_2$ ,  $\text{K}_2\text{TiO}_3$ ,  $\text{SrTiO}_3$  etc., are the wide band gap insulators/semiconductors and hence not suitable for solar energy applications especially visible light photocatalysis. Cadmium sulphide a small band gap semiconductor on the other hand is an efficient visible light photocatalyst [7] but suffers from the problem of photo-corrosion during photochemical reactions [8, 9]. Thus one needs

an efficient photocatalyst that exhibits a high absorption coefficient for visible light photons, as well as being stable against photo-corrosion. The Fe- containing perovskite oxides offer the advantage of high visible light absorptivity by virtue of Fe  $d$ -orbitals/bands in the forbidden region of the band gap. Thus they are one of the best suited absorbers as well as photocatalysts, their abundance and environmentally friendly nature further make them suitable for solar energy conversion materials. Thus we focus our present study on the iron containing metal oxide i.e,  $\text{Sr}_2\text{FeNbO}_6$  system.

In the present study we have synthesized and characterized the SFNO. Further we computed its electronic structure and analysed the results with the experimental observations. It is known [10-16] that a knowledge of the computed electronic structure is an important guide to understand the feasibility of physico-chemical applications. Thus, in the present study we have not only experimentally studied the SFNO system for solar hydrogen generation, but also computed its electronic structure. This demonstrates the suitability of the SFNO system as a well suited visible light photocatalyst for photocatalytic water splitting.

### Experimental

$\text{Sr}_2\text{FeNbO}_6$  was synthesized by the conventional solid-state reaction (SSR) method. Stoichiometric amounts of  $\text{Sr}_2\text{CO}_3$  (99.9%, Aldrich),  $\text{Fe}_2\text{O}_3$  (99%, Aldrich) and  $\text{Nb}_2\text{O}_5$  (99.9%, Aldrich) were mixed and ground in methanol. The pelletized powders were calcined at 973-

\*Corresponding author:

Tel : +82-51-974-6104

Fax: +82-51-974-6116

E-mail: hhgkim@kbsi.re.kr ; phbourse@arci.res.in

1573 K for 5 h in a static furnace. On the other hand, for the purpose of comparison,  $\text{TiO}_{2-x}\text{N}_x$  particles were also prepared by the hydrolytic synthesis method (HSM) [17], in which an aqueous ammonium hydroxide solution with an ammonia content of 28–30% (99.99%, Aldrich) was slowly added drop by drop to a 20% titanium (III) chloride solution ( $\text{TiCl}_3$ , Kanto, contained 0.01% iron as the major impurity) for 30 minute under a  $\text{N}_2$  flow in an ice bath while continuously stirring and the suspension was stirred for 5 h to complete the reaction. After the completion of the reaction, the precipitate was filtered in air and washed several times with deionized water. The filtered powder was dried at 70 °C for 3–4 h in a convection oven. The sample obtained at this stage was an amorphous precipitated power containing ammonia and titanium. Further this sample was calcined at 400 °C for 2 h in an air flow in an electric furnace to obtain crystalline powders of  $\text{TiO}_{2-x}\text{N}_x$ .

The  $\text{Sr}_2\text{FeNbO}_6$  powders thus obtained were characterized by an X-ray diffractometer (Mac Science Co., M18XHF). X-ray diffraction (XRD) results were compared with the Joint Committee Powder Diffraction Standards (JCPDS) data for phase identification. The band gap energy and optical property of the as-prepared materials were measured by a UV-Visible diffuse reflectance spectrometer (Shimadzu, UV 2401).

The photo-reduction reactions of water were carried out at room temperature in an upper-irradiation type Pyrex reaction vessel hooked up into a closed gas circulation system. Photocatalytic reduction was carried out by irradiating the suspended powders using a Hg-arc lamp (500 W) equipped with a cutoff filter ( $\lambda \geq 420$  nm). The  $\text{H}_2$  evolution was examined in an aqueous methanol solution (distilled water 80 ml and  $\text{CH}_3\text{OH}$  20 ml) by stirring 0.3 g of the catalyst loaded with 0.2 wt% Pt. Before the photocatalytic reactions, all the catalysts were loaded with 0.2 wt% Pt using a conventional impregnation method using aqueous  $\text{PtCl}_2$ . The concentration of the reaction product ( $\text{H}_2$ ) was determined by a gas chromatograph equipped with a thermal conductivity detector (a molecular sieve 5-Å column and Ar carrier).

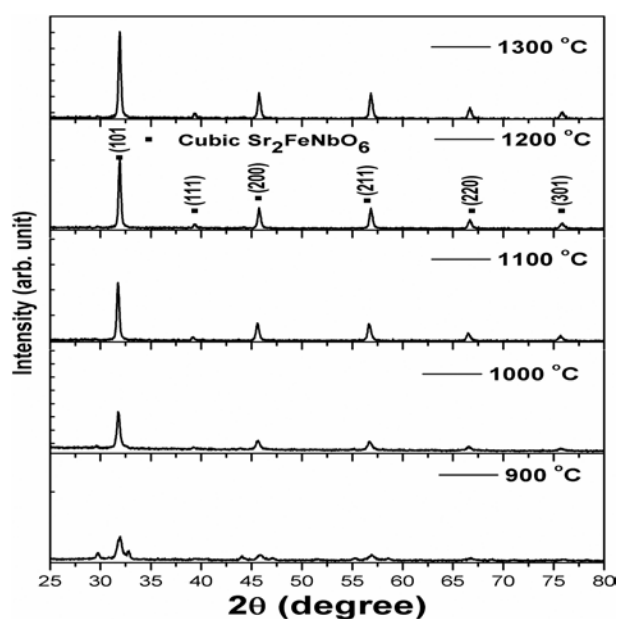
In order to have a qualitative guide, theoretical calculations were performed with the full potential linearized augmented plane-wave (FP-LAPW) method as implemented in the WIEN97 code within density functional theory (DFT) using the Perdew-Wang generalized gradient approximation (GGA) [18]. In the FP-LAPW method the unit cell is divided into two types of regions, the atomic spheres centred upon nuclear sites and the interstitial region between non-overlapping spheres. The potential and charge density are expanded into lattice harmonics and as Fourier series. Thus it is completely general, with no shape approximation for the potential. Calculations carried out at the experimental lattice constant with the atomic coordinates adopted from the literature [19]. It

is noteworthy to say that most of the double perovskite  $\text{Sr}_2\text{FeMO}_6$  (transition metal ions) systems are known frustrated magnetic systems. They are highly complex systems and thus need elaborate studies. As an aim of our paper is to report on photocatalytic hydrogen generation and to the use electronic structure as qualitative guide, we utilized the past basis from a past report to obtain a qualitative picture in the present paper [20]. In addition, the smaller computed band-gap energy is a well-known shortcoming of the single particle Kohn-Sham approach [21]. With this restriction in mind, we performed the present study. We assume that in spite of the limitation with respect to the complexity of this system, the qualitative guide would serve the purpose of a correlation of the experimental data in the present paper. The detailed computation of properties of this system remains a separate elaborate investigation.

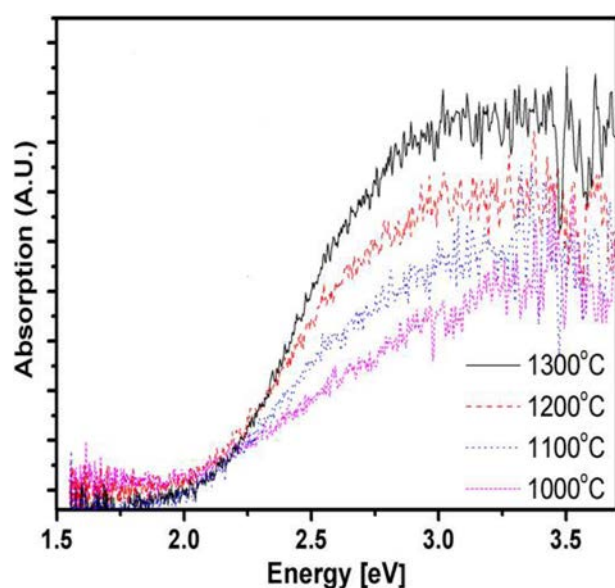
## Results and Discussion

Fig. 1 displays the X-ray diffraction (XRD) spectra of SFNO samples made by the SSR method and calcined at various temperatures. The temperature dependent evolution of the SFNO phase formation can be easily observed from the XRD spectra. The actual onset of the cubic phase formation occurred at around 800 °C, which finally acquired a single phase at 1000 °C. The sample calcined at temperatures  $\geq 1200$  °C were highly crystalline, and exhibited an impurity free, cubic phase [19] having the space group  $Pm-3m$  (lattice constant  $a = 3.97\text{\AA}$ ).

Fig. 2 shows the UV-Vis-DRS spectra for the samples calcined at various temperatures. Experimental results show that the absorption onset edge can be



**Fig. 1.** X-ray diffraction patterns of  $\text{Sr}_2\text{FeNbO}_6$  synthesized by the SSR method and calcined at various temperatures for 10 h.



**Fig. 2.** (Color online) UV-Vis diffuse reflectance spectra for  $\text{Sr}_2\text{FeNbO}_6$  synthesized by the SSR method and calcined at various temperatures for 10 h.

observed for the sample calcined above 1200 °C. The absorption is the result of the contribution due to inter-band transitions along with the possible contribution of Fe-orbitals. The changes in the optical absorption with respect to the samples calcined at different temperatures, are in direct correlation with the crystallinity changes (as estimated by the intensity variation (not shown) of the (101) peak in the X-ray diffraction patterns). It shows an improved crystallinity with an increase in the calcination temperature. This in turn yielded a sharper absorption onset as observed in the optical absorption study. The correlation of structural and optical results affirms that the SFNO is a potential candidate for a visible light absorbing material.

We performed the photo-reduction reaction of water-methanol mixtures under visible light ( $\geq 420$  nm). Fig. 3 shows a comparison of photocatalytic activity of the ferrite system, along with that of the  $\text{PbBi}_2\text{Nb}_2\text{O}_9$  sample [14]. The hydrogen gas evolved over the ferrite sample increased steadily with the reaction time; following this the photoreaction system was evacuated for 5 h in order to remove gaseous products from the gas phase, as shown in Fig. 3. Thus, one can conclude that  $\text{H}_2$  evolution over the photocatalysts occurred photocatalytically. The quantum yield (QY) for the photocatalysts of the material were calculated using the following the equation [15]:

$$\text{QY} = \frac{\text{Rate}(\text{H}_2\text{ evolution})}{12.639} \times \frac{[(I_1 - I_3) - (I_1 - I_2)] \cdot A_1}{A_2} \times 100 \quad (1)$$

where  $I_1$  is the blank light intensity,  $I_2$  is the scattered light intensity,  $I_3$  is the photocatalyst light intensity,  $A_1$

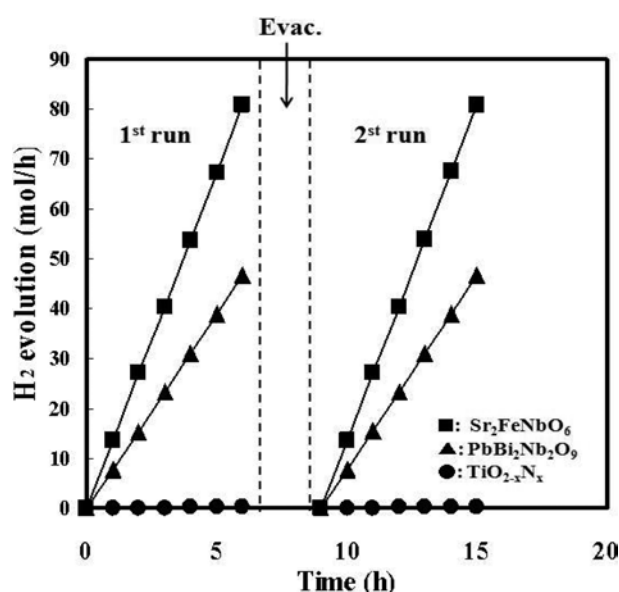


**Fig. 3.** Time course of  $\text{H}_2$  gas evolution from  $\text{Sr}_2\text{FeNbO}_6$ , and  $\text{PbBi}_2\text{Nb}_2\text{O}_9$  (the trace result due to  $\text{TiO}_{2-x}\text{N}_x$  is not shown) under visible light irradiation in an aqueous solution by stirring 0.1 g of catalyst loaded with Pt. The reaction system was evacuated every 5 h in order to remove gaseous products from the gas phase.

**Table 1.** Visible light photocatalytic activities for  $\text{H}_2$  and  $\text{O}_2$  evolution respectively from water-methanol mixtures and silver nitrate solutions over SFNO photo-catalysts.

Catalyst*	Band gap energy		$\text{H}_2$ evolution	
	$E_g$ (eV)	$\lambda$ (nm)	$\mu\text{mol/h}$	QY <sup>a</sup>
$\text{Sr}_2\text{NbFeO}_6$	2.06	600	13.5	1.68
$\text{PbBi}_2\text{Nb}_2\text{O}_9$	2.88	431	7.7	0.9
$\text{TiO}_{2-x}\text{N}_x$	2.73	451	Trace	0

<sup>a</sup>(16)QY: quantum yield

\*Catalyst loaded with 0.1 wt% Pt; 0.3 g; Light source, 450 Watt, Xe-Arc lamp (Oriel) in an inner irradiation quartz cell with a UV cut-off filter ( $\geq 420$  nm). Photoreduction reaction was performed in an aqueous  $\text{CH}_3\text{OH}$  solution [ $\text{CH}_3\text{OH}$  (30 ml) + distilled water (170 ml)].

is the illuminated area of the photoreactor,  $A_2$  is the area of the sensor, and 12.639 is the mole number of photons with  $\lambda \geq 420$  nm emitted from the lamp during 1 h. The estimated QYs of the  $\text{Sr}_2\text{FeNbO}_6$ ,  $\text{PbBi}_2\text{Nb}_2\text{O}_9$  and the  $\text{TiO}_{2-x}\text{N}_x$  photocatalyst [16] are shown in Table 1. The table shows the summarized results to compare and understand the performance of SFNO with respect to standard photocatalysts. It is known that the band energetics of SFNO are favourable for photo reduction and photo oxidation reactions of water [1, 2, 4]. Surprisingly SFNO generated the maximum  $\text{H}_2$  under visible light photons in comparison to the other two systems. Both SFNO and  $\text{PbBi}_2\text{Nb}_2\text{O}_9$  produced  $\text{H}_2$  under visible light photons but  $\text{TiO}_{2-x}\text{N}_x$  produced a trace amount of  $\text{H}_2$ . The difference in the photocatalytic behavior is attributed to the differences in the physicochemical properties of the respective systems,

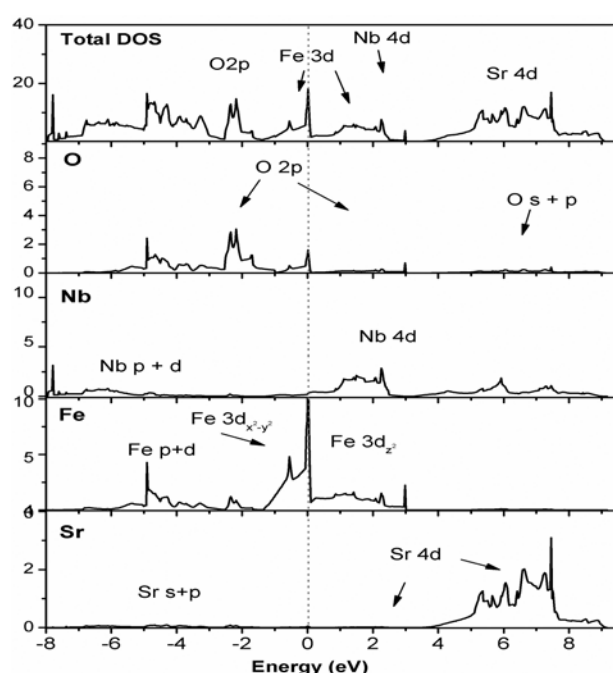


**Fig. 4.** Theoretically calculated total and partial density of states for SFNO. The unit of the Y-axis is states/(eV unit cell). The Fermi level is set at 0 eV.

however in case of SFNO the dominant contributory factors seems to be its electronic property. Here it is noteworthy that as in each case, micrometer sized particulate photocatalysts were synthesized by high temperature calcination, the contribution to the difference in the photocatalytic activity due to the relative differences in the specific surface area will necessarily be negligible.

In order to elucidate the superiority of the SFNO system, we carried out an electronic structure calculation. Fig. 4 shows the calculated total density of states (DOS) alongwith the partial DOS for the cubic SFNO system. It can be observed that Fe-states play a crucial role in the formation of bands in the forbidden gap thereby rendering high visible light absorptivity to the SFNO system. A qualitative analysis of the electronic structure reveals the precise and important role of Fe-atoms in the double perovskite photocatalyst, which can be further used in interpreting the physicochemical behavior of the system. As shown in the Figure, the valence band of SFNO is constituted dominantly by the O  $2p$  states hybridized with Nb-states and additionally the Fe  $3d$  orbitals (Fe  $3d_{x^2-y^2}$ , Fe  $3d_z^2$ ). The conduction band results mainly due to the Sr  $4d$  states, along with minor contribution of the O and Nb states, notably with Nb  $4d$  as its minima. Thus the gap between hybridized the Fe  $d$ -states ( $3d_{x^2-y^2}$  and Fe $3d_z^2$ ) + Nb states near the top of valence band (VB) and the Nb  $4d$  the bottom conduction band (CB) behaves as the band gap of SFNO. Such an electronic structure is responsible for providing a finite probability to inter and intra band transitions. This in turn also affects the absorption

probability of the electrons to low energy (visible radiation) photons. The diffuse reflectance study does validate that the material absorbs visible light photons. Thus one can expect that during the photocatalytic reaction the visible light photons can easily excite the electrons and make them available for the photocatalytic reaction. Thus the electronic structure is crucially decided by the Fe orbitals in the SFNO system under the present study. Effectively SFNO can also become a potential candidate for a solar energy application. The present qualitative guide on one hand shows that Fe plays a vital role in between the valence and conduction band region, similarly experimental observation validates that SFNO efficiently absorbs the visible light photons and yields an efficient photocatalyst for solar hydrogen production.

## Conclusions

The photocatalytic activity for hydrogen (2 times) and oxygen (1.1 times) evolution was very high, as compared to that for  $\text{PbBi}_2\text{Nb}_2\text{O}_9$  (visible light active photocatalysts). Density functional theory of SFNO suggests that the valence band consists of O  $2p$  hybridized with Nb-states and possibly Fe  $3d$  states (Fe  $3d_{x^2-y^2}$ , Fe  $3d_z^2$ ), while the conduction band mainly consists of Sr  $4d$  states, possibly with Nb  $4d$  as its minima. The theoretical and experimental correlation of physicochemical properties of SFNO reveals that Fe-atoms in the cubic lattice of SFNO play a crucial role in yielding high visible light photocatalytic activity.

## Acknowledgements

The authors acknowledge the support of KBSI grant T30320, Hydrogen Energy R&D Center, Korea. One of the authors RD acknowledges the financial support of ARCI, DST lab, Hyderabad, India. The author (PB) also acknowledges the support of Director ARCI, Hyderabad.

## References

1. D.E. Scaife, Solar Energy 25 (1980) 41-54.
2. N. Hatanaka, T. Kobayashi, H. Yoneyama and H. Tamura, Electrochim. Acta 27 (1982) 1129-1133.
3. S. Tao, J. Canales-Vazquez and J.T.S. Irvine, Chem. Mater. 16 (2004) 2309-2316.
4. Y. Matsumoto, J. Solid State. Chem. 126 (1996) 227-234.
5. A. Fujishima and K. Honda, Nature(London) 238 (1972) 37-38.
6. K. Kato and A. Kudo, J. Phys. Chem. B, 106 (2002) 5029-5034.
7. N. Buhler, K. Meier and JP. Reber. J Phys Chem.88 (1984) 3261-3268.
8. A.J. Frank and K. Honda, J Phys Chem. 86 (1982) 1933-1935.
9. D. Meissner, R. Memming and B.Kastening, J Phys Chem. 92 (1988) 3476-3483.
10. S.M. Ji, P.H. Borse, H.G. Kim, D.W. Hwang, J.S. Jang,

- S.W. Bae, J.S. Lee, *Phys. Chem. Chem. Phys.* 7 (2005) 1315-1321.
11. P.H. Borse, H.G. Kim, and J.S. Lee *J. Appl. Phys.* 98 (2005) 043706\_1-4.
12. P.H. Borse, J.S. Lee, and H.G. Kim, *J. Appl. Phys.* 100 (2006) 124915\_1-5.
13. G. Gupta, T. Nautiyal and S. Auluck, *Phys. Rev. B* 69 (2004) 052101\_1-4.
14. H.G. Kim, D.W. Hwang, J.S. Lee, *J. Am. Chem. Soc.* 126 (2004) 8912-8913.
15. S.W. Bae, P.H. Borse, S.J. Hong, J.S. Jang, J.S. Lee, E.D. Jeong, T.E. Hong, J.H. Yoon, J.S. Jin and H.G. Kim, *J. Korean Phys. Soc.* 51 (2007) S22-S26.
16. R. Asahi, T. Morikawa, T. Ohwaki, K. Aoki, Y. Tao, *Science* 293 (2001) 269-271.
17. J.S. Jang, H.G. Kim, S.M. Ji, S.W. Bae, J.H. Jung, B.H. Shon, J.S. Lee, *J. Solid State Chem.* 179 (2006) 1067-1075.
18. P. Blaha, K. Schwarz and J. Luitz, WIEN97, Vienna University of Technology, 1997. Improved and updated Unix version of the original copyrighted WIEN code.
19. M.F. Kupriyanov, and E.G. Fesenko, *Kristallografiya* 6 (1961) 794-796.
20. S. Ray, P. Mahadevan, A. Kumar, D.D. Sarma, R. Cimino, M. Pedio, L. Ferrari, A. Pesci, *Phys. Rev.* 67 (2003) 0851091-6.
21. R.O. Jones and O. Gunnarsson, *Rev. Mod. Phys.* 1989, 61, 689-746.